Search for the Anomalous Events Detected by ANITA Using the Pierre Auger Observatory

A. Abdul Halim,[13] P. Abreu,[73] M. Aglietta,[55,53] I. Allekotte,[1] K. Almeida Cheminant,[71] A. Almela,[7,12] R. Aloisio,[46,47] J. Alvarez-Muñiz,[79] J. Ammerman Yebra,[79] G. A. Anastasi,[59,48] L. Anchordoqui,[86] B. Andrada,[7] S. Andringa,[73] L. Apollonio,[60,50] C. Aramo,[51] P. R. Araújo Ferreira,[43] E. Arnone,[64,53] J. C. Arteaga Velázquez,[68] P. Assis,[73] G. Avila,[11] E. Avocone,[58,47] A. Bakalova,[33] F. Barbato,[46,47] A. Bartz Mocellin,[85] J. A. Bellido,[13,70] C. Berat,[37] M. E. Bertaina,[64,53] G. Bhatta,[71] M. Bianciotto,[64,53] P. L. Biermann,[i] V. Binet,[5] K. Bismark,[40,7] T. Bister,[80,81] J. Biteau,[38,b] J. Blazek,[33] C. Bleve,[37] J. Blümer,[42] M. Boháčová,[33] D. Boncioli,[58,47] C. Bonifazi,[8,27] L. Bonneau Arbeletche,[22] N. Borodai,[71] J. Brack,[k] P. G. Brichetto Orchera,[7] F. L. Briechle,[43] A. Bueno,[78] S. Buitink,[15] M. Buscemi,[48,62] M. Büsken,[40,7] A. Bwembya,[80,81] K. S. Caballero-Mora,[67] S. Cabana-Freire,[79] L. Caccianiga,[60,50] F. Campuzano,[6] I. Caracas,[39,m] R. Caruso,[59,48] A. Castellina,[55,53] F. Catalani,[19] G. Cataldi,[49] L. Cazon,[79] M. Cerda,[10] A. Cermenati,[46,47] J. A. Chinellato,[22] J. Chudoba,[33] L. Chytka,[34] R. W. Clay,[13] A. C. Cobos Cerutti,[6] R. Colalillo,[61,51] M. R. Coluccia,[49] R. Conceição,[73] A. Condorelli,[38] G. Consolati,[50,56] M. Conte,[57,49] F. Convenga,[58,47] D. Correia dos Santos,[29] P. J. Costa,[73] C. E. Covault,[84] M. Cristinziani,[45] C. S. Cruz Sanchez,[3] S. Dasso,[4,2] K. Daumiller,[42] B. R. Dawson,[13] R. M. de Almeida,[29] J. de Jesús,[7,42] S. J. de Jong,[80,81] J. R. T. de Mello Neto,[27,28] I. De Mitri,[46,47] J. de Oliveira,[18] D. de Oliveira Franco,[49] F. de Palma,[57,49] V. de Souza,[20] B. P. de Souza de Errico,[27] E. De Vito,[57,49] A. Del Popolo,[59,48] O. Deligny,[35] N. Denner,[33] L. Deval,[42,7] A. di Matteo,[53] M. Dobre,[74] C. Dobrigkeit,[22] J. C. D'Olivo,[69] L. M. Domingues Mendes,[73,16] Q. Dorosti,[45] J. C. dos Anjos,[16] R. C. dos Anjos,[26] J. Ebr,[33] F. Ellwanger,[42] M. Emam,[80,81] R. Engel,[40,42] I. Epicoco,[57,49] M. Erdmann,[43] A. Etchegoyen,[7,12] C. Evoli,[46,47] H. Falcke,[80,82,81] G. Farrar,[88] A. C. Fauth,[22] N. Fazzini,[g] F. Feldbusch,[41] F. Fenu,[42,f] A. Fernandes,[73] B. Fick,[87] J. M. Figueira,[7] A. Filipčič,[77,76] T. Fitoussi,[42] B. Flaggs,[90] T. Fodran,[80] T. Fujii,[89,h] A. Fuster,[7,12] C. Galea,[80] C. Galelli,[60,50] B. García,[6] C. Gaudu,[39] H. Gemmeke,[41] F. Gesualdi,[7,42] A. Gherghel-Lascu,[74] P. L. Ghia,[35] U. Giaccari,[49] J. Glombitza,[43,d] F. Gobbi,[10] F. Gollan,[7] G. Golup,[1] M. Gómez Berisso,[1] P. F. Gómez Vitale,[11] J. P. Gongora,[11] J. M. González,[1] N. González,[7] D. Góra,[71] A. Gorgi,[55,53] M. Gottowik,[79] T. D. Grubb,[13] F. Guarino,[61,51] G. P. Guedes,[23] E. Guido,[45] L. Gülzow,[42] S. Hahn,[40] P. Hamal,[33] M. R. Hampel,[7] P. Hansen,[3] D. Harari,[1] V. M. Harvey,[13] A. Haungs,[42] T. Hebbeker,[43] C. Hojvat,[g] J. R. Hörandel,[80,81] P. Horvath,[34] M. Hrabovský,[34] T. Huege,[42,15] A. Insolia,[59,48] P. G. Isar,[75] P. Janecek,[33] V. Jilek,[33] J. A. Johnsen,[85] J. Jurysek,[33] K.-H. Kampert,[39] B. Keilhauer,[42] A. Khakurdikar,[80] V. V. Kizakke Covilakam,[7,42] H. O. Klages,[42] M. Kleifges,[41] F. Knapp,[40] J. Köhler,[42] N. Kunka,[41] B. L. Lago,[17] N. Langner,[43] M. A. Leigui de Oliveira,[25] Y. Lema-Capeans,[79] A. Letessier-Selvon,[36] I. Lhenry-Yvon,[35] L. Lopes,[73] L. Lu,[91] Q. Luce,[40] J. P. Lundquist,[76] A. Machado Payeras,[22] M. Majercakova,[33] D. Mandat,[33] B. C. Manning,[13] P. Mantsch,[g] F. M. Mariani,[60,50] A. G. Mariazzi,[3] I. C. Mariş,[14] G. Marsella,[62,48] D. Martello,[57,49] S. Martinelli,[42,7] O. Martínez Bravo,[65] M. A. Martins,[79] M. Mastrodicasa,[46,47,n] H.-J. Mathes,[42] J. Matthews,[a] G. Matthiae,[63,52] E. Mayotte,[85,39] S. Mayotte,[85] P. O. Mazur,[g] G. Medina-Tanco,[69] J. Meinert,[39] D. Melo,[7] A. Menshikov,[41] C. Merx,[42] S. Michal,[33] M. I. Micheletti,[5] L. Miramonti,[60,50] S. Mollerach,[1] F. Montanet,[37] L. Morejon,[39] C. Morello,[55,53] K. Mulrey,[80,81] R. Mussa,[53] W. M. Namasaka,[39] S. Negi,[33] L. Nellen,[69] K. Nguyen,[87] G. Nicora,[9] M. Niechciol,[45] D. Nitz,[87] D. Nosek,[32] V. Novotny,[32] L. Nožka,[34] A. Nucita,[57,49] L. A. Núñez,[31] C. Oliveira,[20] M. Palatka,[33] J. Pallotta,[9] S. Panja,[33] G. Parente,[79] T. Paulsen,[39] J. Pawlowsky,[39] M. Pech,[33] J. Pękala,[71] R. Pelayo,[66] L. A. S. Pereira,[24] E. E. Pereira Martins,[40,7] J. Perez Armand,[21] C. Pérez Bertolli,[7,42] L. Perrone,[57,49] S. Petrera,[46,47] C. Petrucci,[58,47] T. Pierog,[42] M. Pimenta,[73] M. Platino,[7] B. Pont,[80] M. Pothast,[81,80] M. Pourmohammad Shahvar,[62,48] P. Privitera,[89] M. Prouza,[33] S. Querchfeld,[39] J. Rautenberg,[39] D. Ravignani,[7] J. V. Reginatto Akim,[22] M. Reininghaus,[40] J. Ridky,[33] F. Riehn,[79] M. Risse,[45] V. Rizi,[58,47] W. Rodrigues de Carvalho,[80] E. Rodriguez,[7,42] J. Rodriguez Rojo,[11] M. J. Roncoroni,[7] S. Rossoni,[44] M. Roth,[42] E. Roulet,[1] A. C. Rovero,[4] P. Ruehl,[45] A. Saftoiu,[74] M. Saharan,[80] F. Salamida,[58,47] H. Salazar,[65] G. Salina,[52] J. D. Sanabria Gomez,[31] F. Sánchez,[7] E. M. Santos,[21] E. Santos,[33] F. Sarazin,[85] R. Sarmento,[73] R. Sato,[11] P. Savina,[91] C. M. Schäfer,[40] V. Scherini,[57,49] H. Schieler,[42] M. Schimassek,[35] M. Schimp,[39] D. Schmidt,[42] O. Scholten,[15,j] H. Schoorlemmer,[80,81] P. Schovánek,[33] F. G. Schröder,[90,42] J. Schulte,[43] T. Schulz,[42] S. J. Sciutto,[3] M. Scornavacche,[7,42] A. Sedoski,[7] A. Segreto,[54,48] S. Sehgal,[39] S. U. Shivashankara,[76] G. Sigl,[44] G. Silli,[7] O. Sima,[74,c] K. Simkova,[15] F. Simon,[41] R. Smau,[74] R. Šmída,[89] P. Sommers,[l] J. F. Soriano,[86] R. Squartini,[10] M. Stadelmaier,[50,60,42] S. Stanič,[76] J. Stasielak,[71] P. Stassi,[37] S. Strähnz,[40] M. Straub,[43] T. Suomijärvi,[38] A. D. Supanitsky,[7] Z. Svozilikova,[33] Z. Szadkowski,[72] F. Tairli,[13] A. Tapia,[30] C. Taricco,[64,53] C. Timmermans,[81,80] O. Tkachenko,[42] P. Tobiska,[33] C. J. Todero Peixoto,[19] B. Tomé,[73] Z. Torrès,[37] A. Travaini,[10]

P. Travnicek,[33] C. Trimarelli,[58,47] M. Tueros,[3] M. Unger,[42] L. Vaclavek,[34] M. Vacula,[34] J. F. Valdés Galicia,[69] L. Valore,[61,51] E. Varela,[65] A. Vásquez-Ramírez,[31] D. Veberič,[42] C. Ventura,[28] I. D. Vergara Quispe,[3] V. Verzi,[52] J. Vicha,[33] J. Vink,[83] S. Vorobiov,[76] C. Watanabe,[27] A. A. Watson,[e] A. Weindl,[42] L. Wiencke,[85] H. Wilczyński,[71] D. Wittkowski,[39] B. Wundheiler,[7] B. Yue,[39] A. Yushkov,[33] O. Zapparrata,[14] E. Zas,[79] D. Zavrtanik,[76,77] M. Zavrtanik,[77,76]

(Pierre Auger Collaboration)[*]

R. Prechelt,[o] A. Romero-Wolf,[p] S. Wissel,[l] and A. Zeolla[l]

[1]*Centro Atómico Bariloche and Instituto Balseiro (CNEA-UNCuyo-CONICET), San Carlos de Bariloche, Argentina*
[2]*Departamento de Física and Departamento de Ciencias de la Atmósfera y los Océanos, FCEyN, Universidad de Buenos Aires and CONICET, Buenos Aires, Argentina*
[3]*IFLP, Universidad Nacional de La Plata and CONICET, La Plata, Argentina*
[4]*Instituto de Astronomía y Física del Espacio (IAFE, CONICET-UBA), Buenos Aires, Argentina*
[5]*Instituto de Física de Rosario (IFIR)—CONICET/U.N.R. and Facultad de Ciencias Bioquímicas y Farmacéuticas U.N.R., Rosario, Argentina*
[6]*Instituto de Tecnologías en Detección y Astropartículas (CNEA, CONICET, UNSAM), and Universidad Tecnológica Nacional—Facultad Regional Mendoza (CONICET/CNEA), Mendoza, Argentina*
[7]*Instituto de Tecnologías en Detección y Astropartículas (CNEA, CONICET, UNSAM), Buenos Aires, Argentina*
[8]*International Center of Advanced Studies and Instituto de Ciencias Físicas, ECyT-UNSAM and CONICET, Campus Miguelete—San Martín, Buenos Aires, Argentina*
[9]*Laboratorio Atmósfera—Departamento de Investigaciones en Láseres y sus Aplicaciones—UNIDEF (CITEDEF-CONICET), Argentina*
[10]*Observatorio Pierre Auger, Malargüe, Argentina*
[11]*Observatorio Pierre Auger and Comisión Nacional de Energía Atómica, Malargüe, Argentina*
[12]*Universidad Tecnológica Nacional—Facultad Regional Buenos Aires, Buenos Aires, Argentina*
[13]*University of Adelaide, Adelaide, South Australia, Australia*
[14]*Université Libre de Bruxelles (ULB), Brussels, Belgium*
[15]*Vrije Universiteit Brussels, Brussels, Belgium*
[16]*Centro Brasileiro de Pesquisas Fisicas, Rio de Janeiro, Rio de Janeiro, Brazil*
[17]*Centro Federal de Educação Tecnológica Celso Suckow da Fonseca, Petropolis, Brazil*
[18]*Instituto Federal de Educação, Ciência e Tecnologia do Rio de Janeiro (IFRJ), Brazil*
[19]*Universidade de São Paulo, Escola de Engenharia de Lorena, Lorena, Sao Paulo, Brazil*
[20]*Universidade de São Paulo, Instituto de Física de São Carlos, São Carlos, Sao Paulo, Brazil*
[21]*Universidade de São Paulo, Instituto de Física, São Paulo, Sao Paulo, Brazil*
[22]*Universidade Estadual de Campinas (UNICAMP), IFGW, Campinas, Sao Paulo, Brazil*
[23]*Universidade Estadual de Feira de Santana, Feira de Santana, Brazil*
[24]*Universidade Federal de Campina Grande, Centro de Ciencias e Tecnologia, Campina Grande, Brazil*
[25]*Universidade Federal do ABC, Santo André, Sao Paulo, Brazil*
[26]*Universidade Federal do Paraná, Setor Palotina, Palotina, Brazil*
[27]*Universidade Federal do Rio de Janeiro, Instituto de Física, Rio de Janeiro, Rio de Janeiro, Brazil*
[28]*Universidade Federal do Rio de Janeiro (UFRJ), Observatório do Valongo, Rio de Janeiro, Rio de Janeiro, Brazil*
[29]*Universidade Federal Fluminense, EEIMVR, Volta Redonda, Rio de Janeiro, Brazil*
[30]*Universidad de Medellín, Medellín, Colombia*
[31]*Universidad Industrial de Santander, Bucaramanga, Colombia*
[32]*Charles University, Faculty of Mathematics and Physics, Institute of Particle and Nuclear Physics, Prague, Czech Republic*
[33]*Institute of Physics of the Czech Academy of Sciences, Prague, Czech Republic*
[34]*Palacky University, Olomouc, Czech Republic*
[35]*CNRS/IN2P3, IJCLab, Université Paris-Saclay, Orsay, France*
[36]*Laboratoire de Physique Nucléaire et de Hautes Energies (LPNHE), Sorbonne Université, Université de Paris, CNRS-IN2P3, Paris, France*
[37]*Univ. Grenoble Alpes, CNRS, Grenoble Institute of Engineering Univ. Grenoble Alpes, LPSC-IN2P3, 38000 Grenoble, France*
[38]*Université Paris-Saclay, CNRS/IN2P3, IJCLab, Orsay, France*
[39]*Bergische Universität Wuppertal, Department of Physics, Wuppertal, Germany*
[40]*Karlsruhe Institute of Technology (KIT), Institute for Experimental Particle Physics, Karlsruhe, Germany*

[41]Karlsruhe Institute of Technology (KIT), Institut für Prozessdatenverarbeitung und Elektronik, Karlsruhe, Germany
[42]Karlsruhe Institute of Technology (KIT), Institute for Astroparticle Physics, Karlsruhe, Germany
[43]RWTH Aachen University, III. Physikalisches Institut A, Aachen, Germany
[44]Universität Hamburg, II. Institut für Theoretische Physik, Hamburg, Germany
[45]Universität Siegen, Department Physik—Experimentelle Teilchenphysik, Siegen, Germany
[46]Gran Sasso Science Institute, L'Aquila, Italy
[47]INFN Laboratori Nazionali del Gran Sasso, Assergi (L'Aquila), Italy
[48]INFN, Sezione di Catania, Catania, Italy
[49]INFN, Sezione di Lecce, Lecce, Italy
[50]INFN, Sezione di Milano, Milano, Italy
[51]INFN, Sezione di Napoli, Napoli, Italy
[52]INFN, Sezione di Roma "Tor Vergata," Roma, Italy
[53]INFN, Sezione di Torino, Torino, Italy
[54]Istituto di Astrofisica Spaziale e Fisica Cosmica di Palermo (INAF), Palermo, Italy
[55]Osservatorio Astrofisico di Torino (INAF), Torino, Italy
[56]Politecnico di Milano, Dipartimento di Scienze e Tecnologie Aerospaziali, Milano, Italy
[57]Università del Salento, Dipartimento di Matematica e Fisica "E. De Giorgi," Lecce, Italy
[58]Università dell'Aquila, Dipartimento di Scienze Fisiche e Chimiche, L'Aquila, Italy
[59]Università di Catania, Dipartimento di Fisica e Astronomia "Ettore Majorana," Catania, Italy
[60]Università di Milano, Dipartimento di Fisica, Milano, Italy
[61]Università di Napoli "Federico II," Dipartimento di Fisica "Ettore Pancini", Napoli, Italy
[62]Università di Palermo, Dipartimento di Fisica e Chimica "E. Segrè," Palermo, Italy
[63]Università di Roma "Tor Vergata," Dipartimento di Fisica, Roma, Italy
[64]Università Torino, Dipartimento di Fisica, Torino, Italy
[65]Benemérita Universidad Autónoma de Puebla, Puebla, México
[66]Unidad Profesional Interdisciplinaria en Ingeniería y Tecnologías Avanzadas del Instituto Politécnico Nacional (UPIITA-IPN), México, Mexico City, México
[67]Universidad Autónoma de Chiapas, Tuxtla Gutiérrez, Chiapas, México
[68]Universidad Michoacana de San Nicolás de Hidalgo, Morelia, Michoacán, México
[69]Universidad Nacional Autónoma de México, México, Mexico City, México
[70]Universidad Nacional de San Agustin de Arequipa, Facultad de Ciencias Naturales y Formales, Arequipa, Peru
[71]Institute of Nuclear Physics PAN, Krakow, Poland
[72]University of Łódź, Faculty of High-Energy Astrophysics,Łódź, Poland
[73]Laboratório de Instrumentação e Física Experimental de Partículas—LIP and Instituto Superior Técnico—IST, Universidade de Lisboa—UL, Lisboa, Portugal
[74]"Horia Hulubei" National Institute for Physics and Nuclear Engineering, Bucharest-Magurele, Romania
[75]Institute of Space Science, Bucharest-Magurele, Romania
[76]Center for Astrophysics and Cosmology (CAC), University of Nova Gorica, Nova Gorica, Slovenia
[77]Experimental Particle Physics Department, J. Stefan Institute, Ljubljana, Slovenia
[78]Universidad de Granada and C.A.F.P.E., Granada, Spain
[79]Instituto Galego de Física de Altas Enerxías (IGFAE), Universidade de Santiago de Compostela, Santiago de Compostela, Spain
[80]IMAPP, Radboud University Nijmegen, Nijmegen, The Netherlands
[81]Nationaal Instituut voor Kernfysica en Hoge Energie Fysica (NIKHEF), Science Park, Amsterdam, The Netherlands
[82]Stichting Astronomisch Onderzoek in Nederland (ASTRON), Dwingeloo, The Netherlands
[83]Universiteit van Amsterdam, Faculty of Science, Amsterdam, The Netherlands
[84]Case Western Reserve University, Cleveland, Ohio, USA
[85]Colorado School of Mines, Golden, Colorado, USA
[86]Department of Physics and Astronomy, Lehman College, City University of New York, Bronx, New York, USA
[87]Michigan Technological University, Houghton, Michigan, USA
[88]New York University, New York, New York, USA
[89]University of Chicago, Enrico Fermi Institute, Chicago, Illinois, USA
[90]University of Delaware, Department of Physics and Astronomy, Bartol Research Institute, Newark, Delaware, USA
[91]University of Wisconsin-Madison, Department of Physics and WIPAC, Madison, Wisconsin, USA

[*]Contact author: spokespersons@auger.org
[a]Louisiana State University, Baton Rouge, Louisiana, USA.
[b]Institut universitaire de France (IUF), France.
[c]Also at University of Bucharest, Physics Department, Bucharest, Romania.
[d]Present address: ECAP, Erlangen, Germany.

(Received 17 January 2024; revised 29 August 2024; accepted 5 February 2025; published 27 March 2025)

A dedicated search for upward-going air showers at zenith angles exceeding 110° and energies $E > 0.1$ EeV has been performed using the Fluorescence Detector of the Pierre Auger Observatory. The search is motivated by two "anomalous" radio pulses observed by the ANITA flights I and III that appear inconsistent with the standard model of particle physics. Using simulations of both regular cosmic-ray showers and upward-going events, a selection procedure has been defined to separate potential upward-going candidate events and the corresponding exposure has been calculated in the energy range [0.1–33] EeV. One event has been found in the search period between January 1, 2004, and December 31, 2018, consistent with an expected background of 0.27 ± 0.12 events from misreconstructed cosmic-ray showers. This translates to an upper bound on the integral flux of $(7.2 \pm 0.2) \times 10^{-21}$ cm^{-2} sr^{-1} y^{-1} and $(3.6 \pm 0.2) \times 10^{-20}$ cm^{-2} sr^{-1} y^{-1} for an E^{-1} and E^{-2} spectrum, respectively. An upward-going flux of showers normalized to the ANITA observations is shown to predict over 34 events for an E^{-3} spectrum and over 8.1 events for a conservative E^{-5} spectrum, in strong disagreement with the interpretation of the anomalous events as upward-going showers.

DOI: 10.1103/PhysRevLett.134.121003

The Antarctic Impulsive Transient Antenna (ANITA) instruments, flown on long duration NASA balloons at 30–39 km altitudes above Antarctica, have detected radio pulses that are consistent with coherent emission from ultrahigh-energy cosmic-ray (UHECR) air showers. The large horizontal polarization of the pulses is consistent with the geomagnetic effect due to the Earth's magnetic field [1]. The few pulses arriving from directions above the horizon are interpreted as direct emission from air showers with trajectories that do not intercept the surface of the ice (or Earth, in general), here referred to as "Earth-missing showers." The majority of the pulses are reflected at the air-ice interface and appear to arrive from the ice surface (below the horizon). They thus display a characteristic polarity inversion. In addition, several "anomalous" pulses have been reported coming from directions below the horizon [2–4]. These events show strong horizontal polarization, but without the polarity inversion expected for reflected pulses from UHECR showers. The first two such events were detected with the ANITA I and III instruments, respectively, at elevations of 27.4° [2] and 35.0° [3], corresponding to zenith angles of $\theta = 116.7°$ and 124.5° at the intercept of the trajectory with the ice cap. They could be induced by air showers developing in the upward direction, as could be expected from tau lepton decays produced in ultrahigh-energy tau-neutrino interactions below the surface. However, the direction of the observed pulses implies that the neutrinos would need to travel about 6000–7000 km through the Earth before interacting below the ice surface [2]. This corresponds to about 8–10 interaction lengths at the required neutrino energy $E_\nu \gtrsim 0.2$ EeV [5], causing severe attenuation and requiring a ν_τ flux that should have been observed with IceCube and the Pierre Auger Observatory [6–8], the latter being particularly sensitive to Earth-skimming tau neutrinos [9,10]. An astrophysical explanation of the events under standard model (SM) assumptions has also been severely constrained by IceCube [11].

The shower energy inferred from the pulse amplitudes depends on the altitude, h, at which the shower is assumed to start developing with respect to the ice level. Simulated showers injected at $0 < h < 9$ km indicate that the minimum shower energy consistent with the ANITA I (ANITA III) event depends on the unknown shower starting point and is, e.g., ∼0.2 EeV (∼0.15 EeV) for showers starting at $h \sim 5$ km ($h > 5$ km) [6]. Explanations based on subsurface

[e]School of Physics and Astronomy, University of Leeds, Leeds, United Kingdom.
[f]Present address: Agenzia Spaziale Italiana (ASI). Via del Politecnico 00133, Roma, Italy.
[g]Fermi National Accelerator Laboratory, Fermilab, Batavia, IL, USA.
[h]Present address: Graduate School of Science, Osaka Metropolitan University, Osaka, Japan.
[i]Max-Planck-Institut für Radioastronomie, Bonn, Germany.
[j]Also at Kapteyn Institute, University of Groningen, Groningen, The Netherlands.
[k]Colorado State University, Fort Collins, Colorado, USA.
[l]Pennsylvania State University, University Park, Pennsylvania, USA.
[m]Present address: Institute of Physics, University of Mainz, Staudinger Weg 7, D-55099 Mainz, Germany.
[n]Present address: Università di Roma Sapienza and INFN Roma, Italy.
[o]Dept. of Physics and Astronomy, Univ. of Hawai'i, Manoa, Hawaii, USA.
[p]Caltech Jet Propulsion Laboratory, Pasadena, California, USA.

Published by the American Physical Society under the terms of the Creative Commons Attribution 4.0 International license. Further distribution of this work must maintain attribution to the author(s) and the published article's title, journal citation, and DOI.

reflections [12] or coherent transition radiation (TR), expected as an UHECR shower intercepts the ice-air interface, have also been suggested as a possible emission mechanism. TR generated from upward-going showers starting in the ice and intercepting the interface has been ruled out [13], and, similarly, TR due to downward-going UHECR showers intercepting the ice [14] is found to have inconsistent polarity according to recent simulations [15,16].

Given the difficulties in interpreting the anomalous ANITA events, they have attracted a lot of attention. Theoretical interpretations involving physics beyond the SM have been put forward invoking new particles that induce upward-going showers in the atmosphere (see, e.g., [17–23]). Given the relevance of these observations and their discovery potential, a confirmation or a constraint on upward-going air showers from an independent observation is of particular interest. In this Letter, we search for these showers with the Fluorescence Detector of the Pierre Auger Observatory. Similar approaches using optical telescopes were reported in the context of searches for Earth-skimming events induced by interactions of electron neutrinos in the Earth's crust [24] or by tau neutrinos producing taus that decay in flight [25] and are also planned for dedicated future experiments, e.g., [26].

The Pierre Auger Observatory is the largest cosmic-ray detector ever constructed (3000 km^2) for UHECR detection above 0.1 EeV [27,28]. It was completed in 2008 and combines a surface detector (SD), an array of water-Cherenkov detectors to detect the shower front at ground level, and multiple telescopes, known as the Fluorescence Detector (FD), to collect the fluorescence light emitted by nitrogen as the shower front crosses the atmosphere above the SD array. Three high elevation Auger telescopes (HEATs) were added in 2009 to better record low energy showers [29]. UHECR showers typically develop in the downward direction. The timing information from the SD combined with the FD data constitutes a *hybrid* dataset that allows for an improved geometrical reconstruction. The hybrid exposure grows strongly with shower energy, exceeding 300 $\mathrm{km}^2\,\mathrm{sr\,y}$ for 1 EeV [30,31]. That of the FD alone has not been investigated before, but can only be expected to be larger.

Upward-going air showers with zenith angles larger than 110°, as considered here, are unlikely to trigger the SD, so the search presented here uses events having only FD information.

The standard FD reconstruction is carried out in two stages: First, a geometrical reconstruction of the arrival direction and the impact point of the shower on the ground is made using the timing information from the triggered pixels. Second, the signal traces in the pixels are exploited to obtain the development of the energy deposition as a function of the depth of atmosphere traversed, using the Gaisser-Hillas profile [27,32,33].

Alternatively, a global fit (GF) reconstruction is used to simultaneously find the arrival direction, the impact point, and the Gaisser-Hillas energy deposition that best fit the complete pixel data [34]. The analysis takes into account the contribution of scattered Cherenkov light to the signal and it can be used to combine data from several FD locations. As it uses more information, it is more effective in eliminating badly reconstructed events and noise. Both the standard and GF reconstructions are applied in either the upward or downward mode within the OFFLINE analysis framework of the observatory [35].

When the impact point of a shower is in front of a telescope inside the area covered by the SD, as is required for hybrid events, the time sequence of the active pixels clearly defines if it is an upward- or a downward-going event. However, the sequence is reversed if the impact point is behind the telescope (see [36]). When no SD information is available, the reconstruction may be ambiguous with the fits converging in both the upward and downward solutions, one of them being a misreconstruction. Ordinary cosmic-ray showers, which are reconstructed in the upward direction, constitute an unwanted background. This is the case for misreconstructed directions and for some Earth-missing showers that are reconstructed with a zenith angle exceeding 90°, relative to zenith at the center of the SD array.

An important source of background in data is due to laser pulses. Different types of laser shots are routinely fired across the array from different positions at an average rate of about 150 Hz to continuously monitor the atmospheric quality and to test and evaluate the performance of both the FD instrument and the reconstruction procedure [27]. These laser shots naturally mimic showers traveling in the upward direction and are usually precisely time-tagged so that they can be easily vetoed. However, a fraction of order 0.01% of the laser events were not properly labeled and cannot be vetoed. A dedicated effort has been made to identify and discard them by making use of a sample of 10% of the available FD data up to December 31, 2018 ("burn sample"). A set of selection cuts, based on the frequency and location of such events, has been defined to clean the burn sample and, presumably, the full dataset of all laser events.

Dedicated simulations of UHECR (background), as well as upward-going showers (signal), have been produced with CONEX [38] (we use SIBYLL2.3c [39,40] and URQMD1.3 [41] respectively for high and low energy hadronic interactions) to optimize the final search in presence of possible background. For the former, 166×10^6 showers of proton, helium, nitrogen, and iron primaries have been produced in the energy range 0.1–100 EeV. In the first batch, the UHECR-induced showers were isotropically injected over the surface of a sphere of radius 90 km, centered on the array. The zenith angles, θ, relative to zenith at the array center, extend to 100° to include Earth-missing showers. To increase statistics, particularly for inclined events, a second batch of 93×10^6 showers was simulated in the range

60°–100° (where all the background was found in the first batch; cf. [36]. The energy distribution of the full background sample is weighted to mimic the measured UHECR spectrum [30,42].

To study the signal, an isotropic distribution of 6×10^7 upward-going proton showers has been similarly simulated in the range 0.03–10 EeV. We note that, due to shower universality [43], protons stand in for arbitrary primaries with minimal or no loss of generality, since the first interaction points are directly set and all calculations use the shower energy rather than the energy of the primary particle. The combined efficiency for triggering and reconstructing such showers was found to be negligible for energies below 0.03 EeV. The simulated showers are forced to develop at a uniformly distributed altitude above the ground (the altitude of the observatory is taken to be 1400 m above sea level), h, in the range $0 < h < 9$ km with zenith angles, measured at the exit point on the Earth, between 110° and 180°. Altitudes $h > 9$ km are not considered because the exposures of Auger and ANITA fall down rapidly here. This is mostly for geometrical reasons (maximum elevation angles of the Auger FD telescopes and a narrowing Cherenkov cone in case of ANITA). The flat distribution of shower starting points used in the simulations is no restriction, as any distribution can be generated from this by applying corresponding weights to the altitude bins (see below). The ground impact (exit) points have been sampled in a square area of 100×100 km^2 centered on the SD array. This area extends up to ∼20 km behind each FD site to include simulated trajectories with exit points behind the field of view of a telescope [36]. Additionally, to increase statistics in the low energy region, 5×10^6 proton showers have been simulated between 0.1 and 0.3 EeV with impact points contained in a circle with a radius increasing with energy from 12 to 23 km around HEATs but otherwise with the same distributions.

The simulation of the FD signals and trigger, and the subsequent event reconstruction, are done within OFFLINE to study the performance of the reconstruction algorithms. The reconstructed zenith angles correlate well with their true value. However, as no cuts targeted to directional reconstruction precision were applied, a tail in $\theta_{\rm rec} - \theta_{\rm sim}$ is present leading to a 68% central interval of $[-1.1°, 11°]$ (see Ref. [36] for further details).

The selection of candidates compatible with upward-going showers that exit the Earth's surface was performed making use of simulations to reduce the large background to a minimal level. After deciding the entire selection strategy, it was applied to the aforementioned 10% burn sample for verification (see Fig. 1) before it was finally applied blindly to the full FD dataset (7.6×10^6 events). In the first step, the aforementioned laser cuts reduce the data sample to 4.7×10^6 events. To guarantee a minimum data quality [31], only time periods with a clean atmosphere and

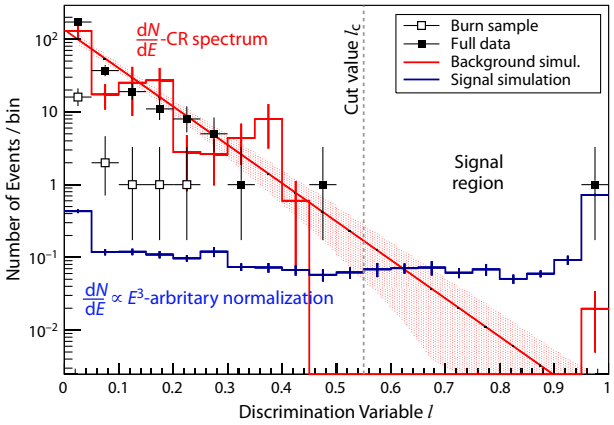

FIG. 1. Distributions of the discriminating variable l, as defined in Eq. (1), for (i) a simulated isotropic background weighted and normalized with the measured UHECR spectrum in the energy range 10^{17} to 10^{20} eV [42] (red histogram with an exponential fit and its uncertainty band); (ii) the signal simulation with energy $10^{16.6}$ to $10^{18.5}$ eV weighted with an E^{-3} spectrum and arbitrarily normalized to one event (blue histogram); and (iii) the data distributions, both for the 10% burn sample and the full dataset (open and filled symbols). The cut value l_c discriminating signal and background is indicated by the vertical dashed line.

low cloud coverage [44], and only events with at least six camera pixels contributing to the time-geometry fit of the shower axis [28] are considered, leaving ∼600 k events. Out of these, 165 000 events can be reconstructed as upward-going in a simple time-geometry fit [28], if only the time sequence and pointing direction of the triggered pixels are considered.

The GF reconstruction is used to check whether the pixel intensity is consistent with a showerlike dE/dX-profile, eliminating many events where the dominant signal is from Cherenkov light. Because of their time-compressed structure they are misreconstructed as upward-going by the simple time fit; cf. [36]. Only 2774 events survive this step. The GF is then also applied in the downward mode and it is found that the majority of the selected events allow both upward and downward reconstructions. Only 986 events are left when two further quality constraints are applied ensuring that the interval of atmospheric slant depth, over which the shower profile is observed, exceeds 80 g cm^{-2} and the reconstructed shower maximum is above ground. To eliminate background from misreconstructed and Earth-missing showers, a cut of $\theta > 110°$ is applied leaving 928 events. Finally, events with $\chi^2_{\rm up} \geq 1.2\chi^2_{\rm down}$ are removed as the downward reconstruction is clearly preferred over the upward reconstruction (the final search criterion, discussed below, is based on comparing the more precise likelihood ratios), reducing the sample to 255 events (cf. Fig. 1). The effects of cuts on data and simulation are compared in the supplemental material.

A search criterion is finally needed to optimize discrimination between upward-going showers (signal) and cosmic-ray events (background). For convenience, we use a function

of the logarithm of the likelihood ratio of the upward and downward modes, $L_{\rm up}/L_{\rm down}$,

$$l = \frac{\arctan\{\ln[\max(L_{\rm up}, L_{\rm down})/L_{\rm down}] \times \zeta\}}{\pi/2}, \quad (1)$$

such that the discrimination variable l ranges from $0 \le l \le 1$, with larger values reflecting larger ratios $L_{\rm up}/L_{\rm down}$. When $L_{\rm down}$ exceeds $L_{\rm up}$, its value is $l = 0$. We note that, occasionally, some simulated cosmic-ray showers can only be reconstructed as upward-going. In such a case, the event is assigned a value of $l = 1$. Finally, the scale parameter ζ in Eq. (1) is chosen such that the signal events uniformly cover the range [0,1]. Figure 1 presents the resulting l distributions for both the UHECR background (red) and the upward-going signal simulations (blue). While the signal distribution is rather flat, the background drops down by about 4 orders of magnitude across the range of l.

A final cut $l > l_c$ is applied to minimize the UHECR background while keeping a sufficiently large fraction of the signal. To optimize l_c, the l distribution of the simulated background has been fitted using several different trial functions. For each fitted distribution, an optimal cut value, l_c, is chosen by performing a scan on l to find the value that minimizes the upper limit obtained for the integral flux of upward-going showers, as discussed below. The flux limit to be minimized in the l_c scan is obtained using an exposure weighted over energy with power laws E^{-1} and E^{-2}, assuming uniform distribution in h and fixing the number of observed events $n_{\rm obs}$ to be equal to the number of events expected from the cosmic-ray background $n_{\rm bkg}$ for a given value of l_c. With these assumptions, the optimal value is found at $l_c = 0.55$ for both considered spectral indices [45]. Above this value, the expected background for the full dataset is $n_{\rm bkg} = 0.27 \pm 0.12$. (We note that all simulated background events passing the l cut in Fig. 1 are found at $l = 1$. They have simulated zenith angles close to 90° and are misreconstructed with $\theta_{\rm rec} > 110°$. See Ref. [36] for further details.) Different parametrizations of the fit to the UHECR background affect the upper limits within 10%. This is included in the quoted uncertainty of the expected background, $n_{\rm bkg}$.

Once a value of l_c is chosen, the full selection and search procedure is completely defined. The sequence of selection cuts is performed on the simulated showers in an identical way as on the data, and it is shown to have similar effects for both [36].

The distribution of events from the full dataset passing the selection criteria agrees well with both the burn sample and the background simulations (cf. Fig. 1 and [36]). After unblinding, one candidate event with $l = 1$ was found, consistent with background expectations, with key features depicted in Fig. 2. Its FD image sweeps a small portion in the top corner of a HEAT camera, triggering only six pixels, i.e., the minimum defined in the quality cuts.

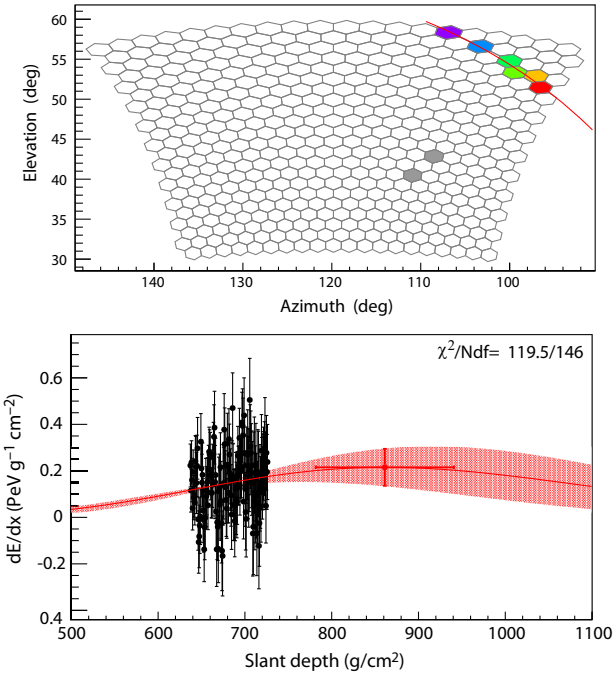

FIG. 2. Remaining event after the selection and search procedure. The top panel shows the triggered pixels of the camera, the earliest one in purple and the last one in red. The bottom plot shows the reconstructed profile that has been fit with the GF reconstruction in the upward-going mode. The time evolution of the signal across a pixel is divided into 50 ns bins to give information from different atmospheric depths.

The reconstruction quality of such events is moderate and in consequence, several poorly imaged events can be found in the background simulations (cf. [36]).

Applying the event selection criteria to the simulated signal allows us to calculate the effective area of the detector for a flux of upward-going air showers as a function of shower energy, E, and starting altitude, h.

An integral flux limit is then obtained by taking the ratio of the maximum number of events allowed by the search to the exposure for selected upcoming showers, $\langle\mathcal{E}\rangle(E > E_0)$, which is weighted with a given energy spectrum. The maximum number of allowed events is taken to be the Rolke limit [46] at 95% CL, $N^{95\%}(n_{\rm bkg}, n_{\rm obs})$, where $n_{\rm obs}$ is the actual number of events observed after unblinding and $n_{\rm bkg}$ the expected number of events for the cosmic-ray background above the specified l_c cut,

$$F^{95\%}(E > E_0) = \frac{N^{95\%}(n_{\rm bkg}, n_{\rm obs})}{\langle\mathcal{E}\rangle(E > E_0)}. \quad (2)$$

Injecting $n_{\rm obs}$ and $n_{\rm bkg}$ from above into this equation and assuming power law spectra E^{-1} and E^{-2} in $E \in [0.1, 33]$ EeV and a distribution uniform in h and isotropic in θ, we find integral flux upper limits at $(7.2 \pm 0.2) \times 10^{-21}$ cm^{-2} sr^{-1} y^{-1} and $(3.6 \pm 0.2) \times 10^{-20}$ cm^{-2} sr^{-1} y^{-1}, respectively. Preliminary results based

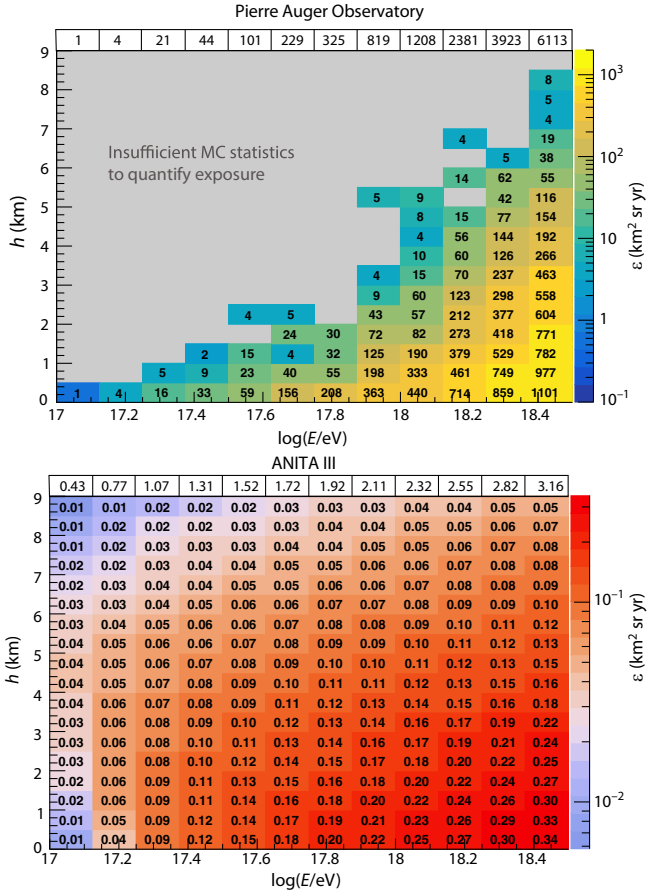

FIG. 3. Exposure of the Auger Observatory (top) and the ANITA III flight (bottom) as a function of shower energy, E, and injection altitude, h, integrated over the zenith angle range $110° \leq \theta \leq 130°$, for an isotropic distribution of arrival directions. The gray area indicates insufficient statistics. In the white cells on top of the exposure plots, we display the sums of the h bins to facilitate comparison (see text).

on lower Monte Carlo statistics and using different energy ranges have been presented in [45,47].

To relate the nonobservation of upward-going showers at the Auger Observatory to the observation of the anomalous events in ANITA, we calculate 2D exposure maps for both observatories as a function of shower energy and shower starting point in the atmosphere. This is done for three zenith angle ranges: 110°–130°, 130°–145°, and 145°–180° and is depicted in Fig. 3 (top) for the first angular bin that largely overlaps with the ANITA anomalous events. The acceptance of the ANITA detector to upward-going showers has been calculated using an analytical approach integrating the surface area and solid angle over a spherical surface concentric with the Earth at altitude h. The accepted solid angle is approximated by the maximum and minimum off-axis angles (of the radio pulse relative to the shower axis) within which the recorded peak amplitude is seen at the detector above a fixed value. These angles are obtained with a set of proton simulations at 0.1 EeV starting at h between 0 and 9 km (above the ice surface) for zenith angles in the range 90°–130° [6]. The pulses are assumed to scale linearly with shower energy. Threshold values of 446 and 284 $\mu V\,m^{-1}$ have been used respectively for ANITA I and III instruments [6]. The exposure for the 110°–130° range in zenith angle has been obtained by multiplying the effective area by the effective flight time, which is 17 (7) days for the ANITA I (III) flight [3,48]. It is displayed in Fig. 3 (bottom) for ANITA III and has been cross-checked modifying a Monte Carlo simulation developed for the calculation of the exposure to tau neutrinos in the ANITA IV flight [49]. (Several authors of this Letter are members of the ANITA Collaboration and have been involved in these calculations.) The two exposures increase with the energy of upward-going showers. That of the Auger Observatory can only be calculated for showers starting at low altitudes, h, because it falls very rapidly with h, and the required simulation statistics become unfeasible to produce, particularly at lower energies. The sums of the exposure bins in h illustrate that the sensitivity of the Auger Observatory exceeds that of the ANITA III flight by factors rising with energy from about 2 to 2000 for a uniform h distribution.

Assuming that the anomalous ANITA events are indeed produced by upward-going showers, we can then calculate the number of upward-going showers expected in the data of the Auger Observatory by convolving a given spectral flux and an h distribution of the showers, with the two 2D exposure maps. Three power law spectra, $E^{-\gamma}$, with $\gamma = 2$, 3, 5 have been assumed, and for each case, we consider both a uniform distribution in h and that expected for exiting taus that decay in the atmosphere. In the latter case, expected from tau-neutrino interactions and in many of the proposed beyond the SM scenarios, the energy E is that of the tau leptons. The starting altitude of the shower strongly depends on zenith angle and tau energy. The required distribution in E and h is obtained from a convolution of the tau flux, the decay-length distribution and the distribution of shower energy for all tau decays as obtained with TAUOLA [50], with an average of ∼50% of the tau energy.

A given energy spectrum can be normalized to the anomalous observations demanding one expected event after folding with the ANITA I or III exposures. Normalizing to ANITA I (III) observation under the assumption of an E^{-3} spectrum and a uniform h distribution, we expect 59 (69) events at the Auger Observatory. Using an h distribution compatible with tau decay reduces expectations to 37 (34) events. Assuming a very conservative spectrum, E^{-5}, to the event of flight I (III) results in 11.7 (8.1) expected events for a uniform h distribution and 18 (11) events for the h distribution expected from tau decay. These numbers are to be compared with one observed event compatible with background. We note that, given a spectral index, the expected number of events obtained using normalizations

from the two flights are similar to one another. The significantly lower signal threshold of the ANITA III instrument is compensated by a lower effective flight duration.

The results of this search do not support the interpretation that the anomalous pulses detected during the ANITA I and III flights were caused by air showers sourced from particle interactions or decays, such as by decays of upward-going taus, the latter being the basis of proposed explanations based on physics beyond the SM. When comparing the results of this study with those reported by ANITA, we note that the exposures of the two detectors have very different dependence on shower altitude. The Auger exposure in the gray area of Fig. 3 (top) is generally below a few $\mathrm{km}^2\,\mathrm{sr\,yr}$ and was set to zero because of insufficient Monte Carlo statistics. However, the large values in the bins at lower altitude overcompensate this effect, unless the showers were distributed exclusively in this yet uncovered region, and/or with mechanisms producing showers with very different longitudinal profiles. No simple mechanism can be anticipated to produce such distributions. It can thus be argued that the upward-going shower explanation is ruled out for a diffuse flux, unless the distribution of the starting altitude of the showers was shaped such that they would only start several kilometers above ground or the shower profiles had unusual shapes. Both would be inconsistent with showers originating from known particle decays or interactions.

Acknowledgments—The successful installation, commissioning, and operation of the Pierre Auger Observatory would not have been possible without the strong commitment and effort from the technical and administrative staff in Malargüe. We are very grateful to the following agencies and organizations for financial support: Argentina—Comisión Nacional de Energía Atómica; Agencia Nacional de Promoción Científica y Tecnológica (ANPCyT); Consejo Nacional de Investigaciones Científicas y Técnicas (CONICET); Gobierno de la Provincia de Mendoza; Municipalidad de Malargüe; NDM Holdings and Valle Las Leñas; in gratitude for their continuing cooperation over land access; Australia—the Australian Research Council; Belgium—Fonds de la Recherche Scientifique (FNRS); Research Foundation Flanders (FWO), Marie Curie Action of the European Union Grant No. 101107047; Brazil—Conselho Nacional de Desenvolvimento Científico e Tecnológico (CNPq); Financiadora de Estudos e Projetos (FINEP); Fundação de Amparo à Pesquisa do Estado de Rio de Janeiro (FAPERJ); São Paulo Research Foundation (FAPESP) Grant No. 2019/10151-2, No. 2010/07359-6, and No. 1999/05404-3; Ministério da Ciência, Tecnologia, Inovações e Comunicações (MCTIC); Czech Republic—GACR 24-13049S, CAS LQ100102401, MEYS LM2023032, CZ.02.1.01/0.0/0.0/16_013/0001402, CZ.02.1.01/0.0/0.0/18_046/0016010, and CZ.02.1.01/0.0/0.0/17_049/0008422 and CZ.02.01.01/00/22_008/0004632; France—Centre de Calcul IN2P3/CNRS; Centre National de la Recherche Scientifique (CNRS); Conseil Régional Ile-de-France; Département Physique Nucléaire et Corpusculaire (PNC-IN2P3/CNRS); Département Sciences de l'Univers (SDU-INSU/CNRS); Institut Lagrange de Paris (ILP) Grant No. LABEX ANR-10-LABX-63 within the Investissements d'Avenir Programme Grant No. ANR-11-IDEX-0004-02; Germany—Bundesministerium für Bildung und Forschung (BMBF); Deutsche Forschungsgemeinschaft (DFG); Finanzministerium Baden-Württemberg; Helmholtz Alliance for Astroparticle Physics (HAP); Helmholtz-Gemeinschaft Deutscher Forschungszentren (HGF); Ministerium für Kultur und Wissenschaft des Landes Nordrhein-Westfalen; Ministerium für Wissenschaft, Forschung und Kunst des Landes Baden-Württemberg; Italy—Istituto Nazionale di Fisica Nucleare (INFN); Istituto Nazionale di Astrofisica (INAF); Ministero dell'Università e della Ricerca (MUR); CETEMPS Center of Excellence; Ministero degli Affari Esteri (MAE), ICSC Centro Nazionale di Ricerca in High Performance Computing, Big Data and Quantum Computing, funded by European Union NextGenerationEU, reference code CN_00000013; México—Consejo Nacional de Ciencia y Tecnología (CONACYT) No. 167733; Universidad Nacional Autónoma de México (UNAM); PAPIIT DGAPA-UNAM; The Netherlands—Ministry of Education, Culture and Science; Netherlands Organisation for Scientific Research (NWO); Dutch national e-infrastructure with the support of SURF Cooperative; Poland—Ministry of Education and Science, Grant No. DIR/WK/2018/11 and 2022/WK/12; National Science Centre, Grant No. 2016/22/M/ST9/00198, No. 2016/23/B/ST9/01635, No. 2020/39/B/ST9/01398, and No. 2022/45/B/ST9/02163; Portugal—Portuguese national funds and FEDER funds within Programa Operacional Factores de Competitividade through Fundação para a Ciência e a Tecnologia (COMPETE); Romania—Ministry of Research, Innovation and Digitization, CNCS-UEFISCDI, Contract No. 30N/2023 under Romanian National Core Program LAPLAS VII, Grant No. PN 23 21 01 02, and Project No. PN-III-P1-1.1-TE-2021-0924/TE57/2022, within PNCDI III; Slovenia—Slovenian Research Agency, Grant No. P1-0031, P1-0385, I0-0033, N1-0111; Spain—Ministerio de Ciencia, 0Innovación y Universidades/Agencia Estatal de Investigación María de Maeztu Grant No. CEX2023-001318-M, N. PID2022-140510NB-I00, No. PCI2023-145952-2 and No. RYC2019-027017-I), Xunta de Galicia (CIGUS Network of Research Centers, Consolidación 2021 GRC GI-2033, ED431C-2021/ 22, and 2022 ED431F-2022/15), Junta de Andalucía (SOMM17/6104/UGR and P18-FR-4314), and the European Union (Marie Skłodowska-Curie 101065027 and ERDF); Junta de Andalucía (SOMM17/6104/UGR and

P18-FR-4314), and the European Union (Marie Skłodowska-Curie 101065027 and ERDF); USA—Department of Energy, Contract No. DE-AC02-07CH11359, No. DE-FR02-04ER41300, No. DE-FG02-99ER41107, and No. DE-SC0011689; National Science Foundation, Grant No. 0450696; The Grainger Foundation; Marie Curie-IRSES/EPLANET; European Particle Physics Latin American Network; and UNESCO.

[1] S. Hoover *et al.* (ANITA Collaboration), Phys. Rev. Lett. **105**, 151101 (2010).
[2] P. W. Gorham *et al.* (ANITA Collaboration), Phys. Rev. Lett. **117**, 071101 (2016).
[3] P. W. Gorham *et al.* (ANITA Collaboration), Phys. Rev. Lett. **121**, 161102 (2018).
[4] P. W. Gorham *et al.* (ANITA Collaboration), Phys. Rev. Lett. **126**, 071103 (2021).
[5] A. Connolly, R. S. Thorne, and D. Waters, Phys. Rev. D **83**, 113009 (2011).
[6] A. Romero-Wolf *et al.*, Phys. Rev. D **99**, 063011 (2019).
[7] I. Safa, A. Pizzuto, C. A. Argüelles, F. Halzen, R. Hussain, A. Kheirandish, and J. Vandenbroucke, J. Cosmol. Astropart. Phys. 01 (2020) 012.
[8] S. Chipman, R. Diesing, M. H. Reno, and I. Sarcevic, Phys. Rev. D **100**, 063011 (2019).
[9] A. Aab *et al.* (Pierre Auger Collaboration), J. Cosmol. Astropart. Phys. 10 (2019) 022.
[10] P. Abreu *et al.* (Pierre Auger Collaboration), Adv. High Energy Phys. **2013**, 708680 (2013).
[11] M. G. Aartsen *et al.* (IceCube Collaboration), Astrophys. J. **892**, 53 (2020).
[12] I. M. Shoemaker, A. Kusenko, P. K. Munneke, A. Romero-Wolf, D. M. Schroeder, and M. J. Siegert, Annals of Glaciology **61**, 92 (2020).
[13] P. Motloch, J. Alvarez-Muñiz, P. Privitera, and E. Zas, Phys. Rev. D **95**, 043004 (2017).
[14] K. D. de Vries and S. Prohira, Phys. Rev. Lett. **123**, 091102 (2019).
[15] J. Ammerman-Yebra, J. Alvarez-Muniz, and E. Zas, Proc. Sci., ICRC2023 (**2023**) 1155.
[16] J. Ammerman-Yebra, J. Alvarez-Muñiz, and E. Zas, J. Cosmol. Astropart. Phys. 04 (2024) 030.
[17] D. B. Fox, S. Sigurdsson, S. Shandera, P. Mészáros, K. Murase, M. Mostafá, and S. Coutu, arXiv:1809.09615.
[18] J. H. Collins, P. S. Bhupal Dev, and Y. Sui, Phys. Rev. D **99**, 043009 (2019).
[19] L. Heurtier, Y. Mambrini, and M. Pierre, Phys. Rev. D **99**, 095014 (2019).
[20] J. M. Cline, C. Gross, and W. Xue, Phys. Rev. D **100**, 015031 (2019).
[21] D. Borah, A. Dasgupta, U. K. Dey, and G. Tomar, Phys. Rev. D **101**, 075039 (2020).
[22] X. Liang and A. Zhitnitsky, Phys. Rev. D **106**, 063022 (2022).
[23] M. H. Reno *et al.*, Phys. Rev. D **105**, 055013 (2022).
[24] R. U. Abbasi *et al.*, Astrophys. J. **684**, 790 (2008).
[25] M. L. Ahnen *et al.* (MAGIC Collaboration), Astropart. Phys. **102**, 77 (2018).
[26] A. N. Otte, Phys. Rev. D **99**, 083012 (2019).
[27] A. Aab *et al.* (Pierre Auger Collaboration), Nucl. Instrum. Methods Phys. Res., Sect. A **798**, 172 (2015).
[28] J. Abraham *et al.* (Pierre Auger Collaboration), Nucl. Instrum. Methods Phys. Res., Sect. A **620**, 227 (2010).
[29] T. H.-J. Mathes (Pierre Auger Collaboration), in *Proceedings of the 32nd International Cosmic Ray Conference* (2011), Vol. 3, p. 153.
[30] P. Abreu *et al.* (Pierre Auger Collaboration), Proc. Sci., ICRC2021 (**2021**) 324.
[31] P. Abreu *et al.* (Pierre Auger Collaboration), Astropart. Phys. **34**, 368 (2011).
[32] T. K. Gaisser and A. M. Hillas, Int. Cosmic Ray Conf. **8**, 353 (1977).
[33] A. Aab *et al.* (Pierre Auger Collaboration), J. Cosmol. Astropart. Phys. 03 (2019) 018.
[34] V. Novotny (Pierre Auger Collaboration), Proc. Sci., ICRC2019 (**2021**) 374.
[35] S. Argiro, S. L. C. Barroso, J. Gonzalez, L. Nellen, T. C. Paul, T. A. Porter, L. Prado, Jr., M. Roth, R. Ulrich, and D. Veberic, Nucl. Instrum. Methods Phys. Res., Sect. A **580**, 1485 (2007).
[36] See Supplemental Material at http://link.aps.org/supplemental/10.1103/PhysRevLett.134.121003, which includes Ref. [37], for examples of signal and background events including Earth-missing showers, details about the reconstruction, and comparisons of the selection procedure for data and for simulated background.
[37] B. Dawson (Pierre Auger Collaboration), Proc. Sci., ICRC2019 (**2020**) 231.
[38] T. Bergmann, R. Engel, D. Heck, N. N. Kalmykov, S. Ostapchenko, T. Pierog, T. Thouw, and K. Werner, Astropart. Phys. **26**, 420 (2007).
[39] F. Riehn, H. P. Dembinski, R. Engel, A. Fedynitch, T. K. Gaisser, and T. Stanev, Proc. Sci., ICRC2017 (**2018**) 301 [arXiv:1709.07227].
[40] E.-J. Ahn, R. Engel, T. K. Gaisser, P. Lipari, and T. Stanev, Phys. Rev. D **80**, 094003 (2009).
[41] S. A. Bass, Prog. Part. Nucl. Phys. **41**, 255 (1998).
[42] A. Aab *et al.* (Pierre Auger Collaboration), Phys. Rev. D **102**, 062005 (2020).
[43] M. Ave, R. Engel, M. Roth, and A. Schulz, Astropart. Phys. **87**, 23 (2017).
[44] A. Aab *et al.* (Pierre Auger Collaboration), Phys. Rev. D **90**, 122005 (2014).
[45] P. Abreu *et al.* (Pierre Auger Collaboration), Proc. Sci., ICRC2021 (**2021**) 1140.
[46] W. A. Rolke, A. M. Lopez, and J. Conrad, Nucl. Instrum. Methods Phys. Res., Sect. A **551**, 493 (2005).
[47] A. Abdul Halim *et al.* (Pierre Auger Collaboration), Proc. Sci., ICRC2023 (**2023**) 1099.
[48] H. Schoorlemmer, K. Belov, A. Romero-Wolf, D. García-Fernández, V. Bugaev, S. Wissel, P. Allison, J. Alvarez-Muñiz, S. Barwick, J. Beatty *et al.*, Astropart. Phys. **77**, 32 (2016).
[49] R. Prechelt *et al.* (ANITA Collaboration), Phys. Rev. D **105**, 042001 (2022).
[50] M. Chrzaszcz, T. Przedzinski, Z. Was, and J. Zaremba, Comput. Phys. Commun. **232**, 220 (2018).